



(51) International Patent Classification:
G01T 1/29 (2006.01) A61N 5/10 (2006.01)

(21) International Application Number:
PCT/IB2019/050258

(22) International Filing Date:
14 January 2019 (14.01.2019)

(25) Filing Language: Italian

(26) Publication Language: English

(30) Priority Data:
102018000000867 15 January 2018 (15.01.2018) IT

(71) Applicants: UNIVERSITA' DI PISA [IT/IT]; Lungarno Pacinotti 43/44, I-56126 Pisa (IT). ISTITUTO NAZIONALE DI FISICA NUCLEARE [IT/IT]; Via E. Fermi 40, I-00044 Frascati (Roma) (IT).

(72) Inventors: SPORTELLI, Giancarlo; Via Antonio Guadagnoli 9, I-56124 Pisa (IT). BISOGNI, Maria Giuseppina; Via S.A. Pucci 89, I-55049 Viareggio (Lucca) (IT). KOSTARA, Eleftheria; GR-30011 Zevgaraki (Agrinio) (GR). MORROCCHI, Matteo; Via Sante Tani 10, I-56123 Pisa (IT). CAMARLINGHI, Niccolò; Piazzale Martin Luther King 1, I-56123 Pisa (IT).

(74) Agent: VANZINI, Christian et al.; c/o Jacobacci & Partners S.p.A., Corso Emilia 8, 10152 Torino (IT).

(81) Designated States (unless otherwise indicated, for every kind of national protection available): AE, AG, AL, AM, AO, AT, AU, AZ, BA, BB, BG, BH, BN, BR, BW, BY, BZ, CA, CH, CL, CN, CO, CR, CU, CZ, DE, DJ, DK, DM, DO, DZ, EC, EE, EG, ES, FI, GB, GD, GE, GH, GM, GT, HN, HR, HU, ID, IL, IN, IR, IS, JO, JP, KE, KG, KH, KN, KP, KR, KW, KZ, LA, LC, LK, LR, LS, LU, LY, MA, MD, ME, MG, MK, MN, MW, MX, MY, MZ, NA, NG, NI, NO, NZ,

(54) Title: METHOD AND APPARATUS FOR ACQUIRING POSITRON EMISSION TOMOGRAPHY DATA IN FULL BEAM HADRON THERAPY

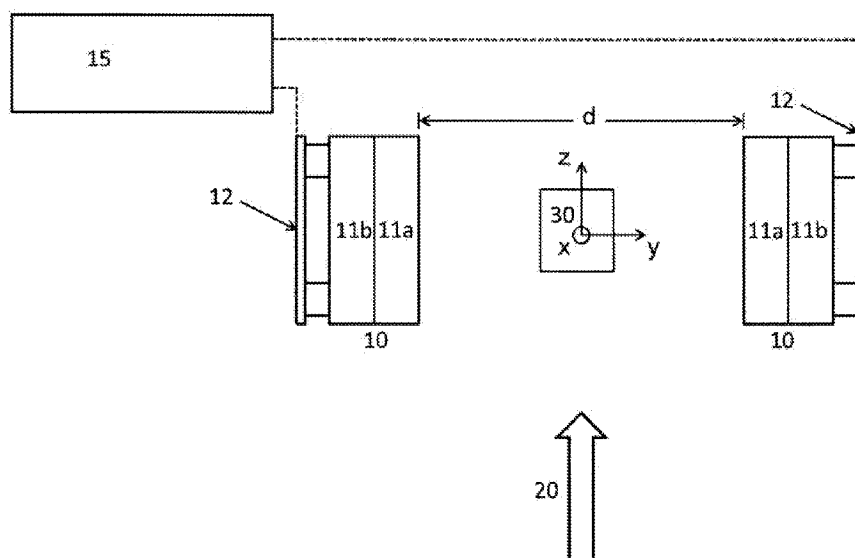


FIG. 1

(57) Abstract: Apparatus for acquiring positron emission tomography data when irradiating an object (20) with a hadron beam (B), the apparatus comprising a plurality of detectors (10) and a data processing system (12, 15). The data processing system (12, 15) is configured to process the detection data according to the following steps: a) determining a temporal distribution of the coincidence event rate acquired by the respective detector (10), b) sampling each spill interval with a sampling frequency of the order of magnitude of GHz to obtain a respective fine grained event rate distribution; c) for each spill interval: - c1) analysing frequencies of the fine grained event rate distribution to find an initial frequency value f_0 compatible with the radiofrequency signal of the hadron beam; - c2) from the initial frequency value, estimating period T_s of the micro-bunches and transforming time values of the coincidence events in the spill interval into values of phase relative to an arbitrary phase, based on the estimated period of the micro-bunches; and - c3) at each



OM, PA, PE, PG, PH, PL, PT, QA, RO, RS, RU, RW, SA, SC, SD, SE, SG, SK, SL, SM, ST, SV, SY, TH, TJ, TM, TN, TR, TT, TZ, UA, UG, US, UZ, VC, VN, ZA, ZM, ZW.

- (84) Designated States** (*unless otherwise indicated, for every kind of regional protection available*): ARIPO (BW, GH, GM, KE, LR, LS, MW, MZ, NA, RW, SD, SL, ST, SZ, TZ, UG, ZM, ZW), Eurasian (AM, AZ, BY, KG, KZ, RU, TJ, TM), European (AL, AT, BE, BG, CH, CY, CZ, DE, DK, EE, ES, FI, FR, GB, GR, HR, HU, IE, IS, IT, LT, LU, LV, MC, MK, MT, NL, NO, PL, PT, RO, RS, SE, SI, SK, SM, TR), OAPI (BF, BJ, CF, CG, CI, CM, GA, GN, GQ, GW, KM, ML, MR, NE, SN, TD, TG).

Declarations under Rule 4.17:

- *as to applicant's entitlement to apply for and be granted a patent (Rule 4.17(ii))*
- *of inventorship (Rule 4.17(iv))*

Published:

- *with international search report (Art. 21(3))*

Method and apparatus for acquiring positron emission tomography data in full beam hadron therapy

The work leading to this invention has received funding from the People Programme (Marie Curie Actions) of the European Union's Seventh Framework Programme (FP7/2007-2013) under REA grant agreement n° 317446.

The present invention relates in general to techniques for data acquisition for positron emission tomography (PET) for in-beam monitoring in hadron therapy.

10

In oncological hadron therapy, proton beams or light ions (hadrons) are accelerated so as to strike and damage tumour tissues in the patient. A characteristic of the therapy is that the hadrons release most of their energy in a very precise point of their trajectory (the Bragg peak), depending on their initial energy. Outside the Bragg peak, energy and therefore damage to healthy tissues is less than conventional radiation therapy. This allows the tumour areas to be damaged with great precision, thus saving healthy ones around them. Since the position of the Bragg peak also depends on physiological parameters and the conformation of the tissue traversed by the beam, in order to fully exploit the potential of the hadron therapy, a monitoring system is necessary that allows verifying that the Bragg peak is in the predetermined position. Technically, this type of operation is called verification of the beam range.

15
20

In the last 15 years, different methods of range verification have been developed, the most mature of which is the use of PET to visualize the trace of radioactive isotopes left by the hadron beam during its path towards the Bragg peak. The PET for the verification of the range is distinguished in: off-line, when the patient is transported from the treatment room to a room equipped with conventional PET; in-room, when the conventional PET system is installed in the same treatment room; in-beam, when a dedicated PET system is installed on the treatment table or integrated into the beam delivery gantry.

25
30

The in-beam option is the most effective but also the most difficult to implement. In particular, it is not convenient in the prior art to acquire sensitive PET data while the beam is

on, that is, when the PET signal is as high as possible, since also the noise due to the products of the nuclear interactions of the beam is very high. The intensity of the noise from the light beam depends on the timing accuracy of the acquisition system and can be reduced within the limits of the acquisition technology used (G. Sportelli et al., 2014, "First full-
5 beam PET acquisitions in proton therapy with a modular dual-head dedicated system". *Physics in Medicine and Biology* 59, 43–60). To overcome this drawback, two solutions have been proposed in the past in which the PET system synchronizes with the RF frequency of the beam and discards all the data that were acquired during the step of extraction of the particles (in which the noise is maximum) and maintains the data acquired during
10 the particle acceleration step (in which the noise is minimal) (P. Crespo et al., 2005, "Suppression of random coincidences during in-beam PET measurements at ion beam radiotherapy facilities", *IEEE transactions on nuclear science*, 52-4:980-987). The background noise is in fact periodic and is concentrated in a phase window (dependent on the energy of the beam) with respect to the period of the RF signal of the accelerator (K.
15 Parodi et al., 2005, "Random coincidences during in-beam PET measurements at microbunched therapeutic ion beams", *Nuclear Instruments and Methods in Physics Research Section A: Accelerators, Spectrometers, Detectors and Associated Equipment* 545, 446–458). Note that the dependence of the arrival time of the particles with respect to their energy depends on the fact that the velocity of the particles is related to their kinetic energy.

20

In a practical implementation, the above synchronization is achieved 1) by exploiting the accelerator RF signal or 2) by means of a particle detector positioned on the beam line. The first solution requires hardware designed to integrate the PET system with the accelerator and offers good performance when the beam is monoenergetic, but is not usable in the clinic
25 with beams at different energies, because it does not correct for the dependence of the arrival time from the energy. The second solution also requires dedicated hardware placed in the same beam line and provides a more faithful signal to the arrival time of the particles (the space travelled by the detector to the target will cause a residual time error depending on the energy). The need to pass the beam through a dedicated detector, however, poses
30 additional problems for commissioning the beam and provides a signal to noise ratio that is too low to be used for practical purposes (P. Crespo et al., 2005, *ibidem*).

An object of the present invention is to propose an alternative technique for synchronizing the PET system and the accelerator, which is not affected by the drawbacks of the known solutions discussed above.

5 To this end, the object of the invention is an apparatus for acquiring positron emission tomography data when irradiating an object with a hadron beam, said apparatus comprising:

a plurality of detectors configured to detect radiation emitted by the object when irradiating it with the hadron beam, and provide detection data; and

10 a data processing system configured to reconstruct positron emission tomography imaging data from the detection data provided by the detectors, and determine the penetration range of the hadron beam in the object;

wherein the data processing system is configured to process the detection data according to the following steps:

15 a) determining a time distribution of the rate of coincidence events acquired by the respective detector (hereinafter also referred to as "event rate"), said time distribution having a succession of spill intervals correlated with a pulsed time structure of the hadron beam, each spill interval having a micro-structure formed by a succession of micro-bunches correlated with a radiofrequency signal of the hadron beam;

20 b) sampling each spill interval with a sampling frequency of the order of magnitude of GHz to obtain a respective fine grained event rate distribution;

c) for each spill interval:

- c1) analysing frequencies of the fine grained event rate distribution to find an initial frequency value f_0 compatible with the radiofrequency signal of the hadron beam;

25 - c2) from the initial frequency value, estimating period T_s of the micro-bunches and transforming time values of the coincidence events in the spill interval into values of phase relative to an arbitrary phase, based on the estimated period of the micro-bunches; and

- c3) at each micro-bunch of the spill interval, executing filtering to remove coincidence events around a peak associated with background noise induced by the hadron beam and keep the remaining coincidence events of the micro-bunch.

30

In particular, step c1) may comprise

calculating a fast Fourier transform of the fine grained event rate distribution.

In particular, step c2) may comprise

determining, in the fast Fourier transform, the frequency f_0 of the first peak with non-zero frequency;

determining an initial value T_0 of the period, where $T_0 = 1/f_0$;

5 assigning to each coincidence event a phase value ϕ_i based on the initial value T_0 of the period such that

$$\phi_i = t_i \bmod T_0, \quad (1)$$

where t_i is the timestamp of the i -th event and mod is the modulus operator; and

iteratively searching for the period T_j around T_0 that maximizes the peak-to-valley
10 ratio of the event rate over the period, to obtain the best estimate T_s of the period of the micro-bunches.

In particular, step c3) may comprise

determining mean μ and standard deviation σ of a Gaussian fit applied to the peak
15 associated with background noise induced by the hadron beam; and

removing the coincidence events comprised in the interval $\mu \pm k\sigma$, where k is an adjustable arbitrary number.

Preferably, the sampling frequency is between 1 and 10 GHz.

20

A further object of the invention is a method for acquiring positron emission tomography data during the irradiation of a phantom with a hadron beam, said method comprising:

detecting radiation emitted by the phantom when irradiating it with the hadron beam, and providing detection data; and

25 reconstructing positron emission tomography imaging data from the provided detection data, and determining the penetration range of the hadron beam in the phantom;

wherein the detection data are processed according to the following steps:

a) determining a time distribution of the event rate of coincidence events acquired by the respective detector, said time distribution having a succession of spill intervals correlated
30 with a pulsed time structure of the hadron beam, each spill interval having a micro-structure formed by a succession of micro-bunches correlated with a radiofrequency signal of the hadron beam;

b) sampling each spill interval with a sampling frequency of the order of magnitude of GHz to obtain a respective fine grained event rate distribution;

c) for each spill interval:

- c1) analysing frequencies of the fine grained event rate distribution to find an initial frequency value f_0 compatible with the radiofrequency signal of the hadron beam;
- c2) from the initial frequency value, estimating period T_s of the micro-bunches and transforming time values of the coincidence events in the spill interval into values of phase relative to an arbitrary phase, based on the estimated period of the micro-bunches; and
- c3) at each micro-bunch of the spill interval, executing filtering to remove coincidence events around a peak associated with background noise induced by the hadron beam and keep the remaining coincidence events of the micro-bunch.

The invention uses the temporal micro-structure observed in the events detected by the PET acquisition system. Experimental data have in fact shown that the acquired positron-electron annihilation photons have a temporal distribution with the same periodicity of the acceleration/extraction cycle of the accelerator. By the invention it is therefore possible to acquire data in shorter times (with full-beam) and to reproduce images with a signal/noise ratio better than the prior art. The monitoring operation is also less invasive, as it does not require the patient to remain immobile for a long time after treatment to allow the PET acquisition.

Further features and advantages of the invention will become apparent from the following detailed description of an embodiment of the invention, made with reference to the accompanying drawings, provided for illustrative and non-limiting purposes only, in which

figure 1 is a diagram representing a PET apparatus;

figure 2 is a diagram of the data processing of the method according to the invention;

figure 3 shows: a) expected distribution of fine-grained event rate for a spill interval, using data of a fraction of the spill interval. The considered spill interval has a duration of 1 s. The illustrated fraction has dimension $[Ofs, Ofs+W)$, where $Ofs=2$ ms and $W=8$ ms. The sampling intervals of the fine-grained event rate have amplitude equal to $t_s=1$ ns; b) a magnification of a part of the distribution a). Note that most sampling intervals contain no events;

figure 4 represents the FFT diagram of a spill interval. The first highest peak (except for the zero frequency peak) provides the main frequency $f_0=1.666$ MHz, compatible with the accelerator radiofrequency. The period is calculated from $T_0=1/f_0=600.2$ ns;

figure 5 shows the histogram of the event steps for the micro-bunches of a spill interval: a) when the period $T_0=600.2$ ns is calculated by FFT; when the period is iteratively estimated in the interval $[T_0\pm 200$ ps] with a step of 0.5 ps, such that: b) $T_1=600.21$ ns and c) $T_2=600.216$ ns, obtaining the best estimate d) $T_s=695.2165$ ns;

figure 6 represents the Gaussian fit on the peak of the micro-bunch to define a window around the peak and keep the data outside the defined window. These data correspond to coincidence events during the pauses between the micro-bunches, indicated as in-spill inter-bunch data;

figure 7 represents the image reconstruction of a) inter-spill coincidence events; b) in-spill coincidence events; c) in-spill inter-bunch coincidence events (after filtering); using the central slice in the x-z plane of the spatial distribution of the coincidence events. The direction of the beam is from left to right. In b), the background radiation noise induced by the beam is visible with the detection of coincidence events before the input surface of the phantom and at the end of the image. In c), the noisy background in the reconstructed image is significantly lower than in b); and

figure 8 shows the one-dimensional profiles of: a) inter-spill coincidence events; b) in-spill coincidence events; c) in-spill inter-bunch coincidence events (after filtering). In b), the background radiation noise induced by the beam is visible in the high activity before the input surface of the phantom and in the tail at the end of the activity interval. In c), the number of coincidence events before the input surface of the phantom decreases significantly. The tail at the end of the activity interval does not change.

The invention will now be described with reference to a PET detector represented schematically in figure 1. It is understood, of course, that the invention is not limited to this specific example, but is applicable to any type of PET detector.

The PET detector in figure 1 consists of two detection modules 10, located at a distance d from each other. As an example, the detection modules may have a dimension of 5 cm x 5 cm, and may be arranged at a distance of 50 cm. In this case, the scintillator array can be

composed, for example, of 20 x 20 pixels of LSO of thickness 2 cm and section 2.5 mm x 2.5 mm. Each module consists of an array of scintillator crystals 11a coupled with photo-detectors 11b (e.g. silicon photomultipliers - SiPM). Each photo-detector is read by a front-end electronics 12 which provides for each event the energy released in the crystal and the interaction time. The measurement can take place, for example, via an application-specific integrated circuit (ASIC). A back-end computer 15 is operatively connected with the front-end boards 12 to receive the processed detection data and to reconstruct, from them, image data for positron emission tomography, as well as to determine the penetration range of the Hadron beam, in a conventional manner. The process of processing the detection data by the electronics of the front-end cards 12, shown in figure 2, will be described below.

The beam of particles 20 impinges on a phantom 30 arriving parallel to the z axis, if a synchrotron beam is used, the irradiation sequence consists of on-beam intervals followed by off-beam intervals. In the following, the on-beam intervals will also be indicated as spill or spill intervals. The events detected in the spill will be indicated as in-spill events, while the events detected in the off-beam intervals will be indicated as inter-spill events. The events acquired as a result of the irradiation due to the residual activity inside the phantom will be indicated as post-irradiation events.

The scanned data is saved sequentially in a file and includes in-spill, inter-spill and post-irradiation events. For each event the time stamp, there are given the energy released (some techniques for the identification of the energy of the event include time-over-threshold, peak detection, charge integration), the unique identifier of the photo-detector that has acquired the event, and possibly the detection position in the photo-detector from which it is possible to identify the scintillator crystal in which the photon has interacted. It is specified that the invention is not limited to the use of crystal arrays, but can also be implemented with continuous scintillating crystals in which the position of the annihilation photon interaction with the crystal is determined by processing the shape of the light distribution on the photo-detector.

30

The distribution of the event rate as a function of time depends on the pulsed temporal structure of the beam. The distribution is used to pre-process the data and identify the be-

ginning and end of each spill, which allows the in-spill data to be separated from the inter-spill data.

For the reconstruction of the PET image, events around the peak of annihilation of 511 keV are used. The selection of energy windows can be made taking into account the local non-uniformities of the crystal, the photo-detector and the portion of front-end electronics involved in the interaction. For this purpose, post-irradiation data are used and prompt coincidences are defined. Then, the energy spectrum is analysed and a Gaussian fit is applied to the peak of 511 keV. The parameters of the Gaussian fit, mean μ and standard deviation σ , are saved in separate files for each front-end electronics channel and used to define an energy window around the peak (equal, for example, to $\mu \pm 3\sigma$). The energy window is not necessarily the same for each channel and is applied to the data in order to keep events around the peak of 511 keV, discarding the rest. Note that it is possible to define other metrics to determine which events to filter, for example using both the phase value and the energy of each event, without necessarily resorting to a Gaussian fit. For example, events with certain energies could be accepted on narrower time frames than events with other energies.

An initial analysis is performed using inter-spill and in-spill data. First the prompt coincidences are calculated, determining for each coincidence the two positions of interaction with the detector and the line connecting the two, called the response line.

The images are then reconstructed using a reconstruction algorithm, such as the "Maximum Likelihood Expectation Maximization" (ML-EM). Let's consider, for example, the central slice in the x-z plane of the three-dimensional (3D) spatial distribution of the coincidence events of the reconstructed image.

The one-dimensional activity profile (1D) is defined as the intensity of the voxel along the beam direction of the 3D image slice that passes through the isocenter and is parallel to the two sensing modules considered in this example. To reduce statistical fluctuations, the 1D activity profile can be obtained by averaging several slices around the central slice along the x direction. The activity range is measured from the 1D activity profile.

It is known that the beam microstructure has a strong correlation with the radiofrequency (RF) signal of the accelerator (Parodi et al., 2005, *ibidem*). Each spill is characterized by bunches of tens of nanoseconds, at equal distance from each other over time according to the RF period of the accelerator. Data are analysed separately for spill due to small differences in their internal microstructure.

For each spill, the fine grained event rate (FGER) is calculated, i.e. the number of events that fall in very short time intervals, in the order of 1 ns. Although it is a highly inaccurate estimate of the instantaneous event rate, the FGER still contains the temporal properties to be extracted from the data. It can be expected that by analysing the frequencies of the FGER, e.g. by applying a fast Fourier transform (FFT), a component corresponding to the radiofrequency of the accelerator is found. The result of the FFT would show a peak at zero frequency, corresponding to the average event rate over the entire spill interval, and another at the frequency f_0 corresponding to the accelerator radiofrequency. Once you have found f_0 looking for the first FFT peak after the continuous level, you can estimate the main RF period $T_0=1/f_0$. Furthermore, based on the estimate, a phase value ϕ_i can be assigned to each event with respect to this period:

$$\phi_i = t_i \bmod T_0, \quad (1)$$

where t_i is the timestamp of the i -th event and mod is the modulus operator. Knowing the phases of the events, we could calculate the histogram of these phases and derive the probability of an event occurring in different phase intervals of the period, in a way that resembles the intensity of the micro-bunch published in (Parodi et al., 2005, *ibidem*), Random coincidences during in-beam PET measurements at microbunched therapeutic ion beams, Nuclear Instruments and Methods in Physics Research Section A: Accelerators, Spectrometers, Detectors and Associated Equipment, 545(1):446-458. The form of the micro-bunch thus derived depends strongly on the accuracy of the estimate of the period. In fact, the error of drift on the estimation of the phases due to the inaccuracies of the period accumulates over time and limits the ability to analyse long acquisition intervals together. This effect can be mitigated by searching iteratively for the period T_j around T_0 which maximizes the peak-to-down ratio of the phases over the period. This was done on the experimental data by applying function (1) for different values of T_j in the interval $[T_{(j-1)}, t_r]$, where t_r is reduced to each iteration j , and thus providing the best estimate of the micro-

bunch period (T_s).

A phase offset is also added to confine the ascending and descending fronts of the same micro-bunch in the period:

$$5 \quad \phi_i = t_i \bmod T_s, + \phi_b, \quad (2)$$

where t_i is the time stamp of the i -th event, T_s is the best estimate of the micro-bunch period and ϕ_b is the phase offset. The phase offset is selected so as to have the micro-bunch substantially centred in the period.

10 It is known that the background noise induced by the beam cannot be separated from the coincidentally usable events, originating from the decays of the β^+ emitters, with the standard techniques of correction of accidental coincidences. Consequently, in order to operate in-spill, it is necessary to estimate the high number of random counts with a different method.

15

According to the invention, in-spill data is filtered to remove the noise events that accumulate at the micro-bunch passing through the target. This is done in a similar way to what has already been done in (P. Crespo et al., 2005, *ibidem*). Using the best estimate of the period, T_s , a Gaussian fit is applied to the peak to represent micro-bunches of the spill. The parameters of the Gaussian fit, mean μ and standard deviation σ , are saved for each spill. A window is then established around the peak of the spill. In this way, the coincidence events that occur in the micro-bunches, in the defined window, are removed and only the events during the pauses between the micro-bunches are selected, which will be indicated below as inter-bunch in-spill data.

25

The FGER is presented in figure 3. As already mentioned, the detected events are temporally scattered, and consequently the number of events in each container will be extremely small. This is shown in figure 3a, which shows that the maximum number of counts per sampling interval is three. In figure 3b, which shows an enlarged part of the FGER, it is shown that a significantly large number of containers do not contain any event.

30

The result of the FFT implementation of FGER is shown in figure 4. The highest peak at

non-zero frequency is the one which gives the main frequency f_0 , which in the selected spill is equal to $f_0=1.666$ MHz and is compatible with the frequency of the accelerator used. Consequently, the period $T_0=1/f_0$ is equal to $T_0=600.2$ ns.

5 This value is used as the starting value for the calculation of the micro-bunch histogram. Thus, the algorithm searches around T_0 in the interval $[T_0 \pm 200$ ps], using a step of 0.5 ps to maximize the peak of the histogram. Note that the magnitude of the search interval of the optimal period and the search step can be varied to optimize the search times and the accuracy of the result. Figure 5a shows the micro-bunch obtained using the period $T_0=$
10 600.2 ns as directly calculated by the FFT. Figure 5d shows the best estimate of the period with a seven-digit precision, $T_s=600.2165$ ns. the optimization of the period leads to the minimization of the FWHM of the micro-bunch distribution. Figures 5b and 5c show the representation of the micro-bunch in two intermediate estimates of the period, $T_1=600.21$ ns and $T_2=600.216$ ns.

15

Figure 6 shows a Gaussian fit applied to the peak as described above. The window around the peak of the spill is equal to $\mu \pm 2\sigma$. Discarding data within this window removes more than 65% of the total coincidence events in the spills.

20 Figures 7a and 7b show the reconstructed images of inter-spill and in-spill data. The beam enters from the left side. The in-spill distribution is noisier than inter-spill distribution. This happens because of the limited statistics during the spill, which occupies a fraction equal to 20% of the entire acquisition time in the image. In particular, in figure 7b it can be seen that coincidence events are present before the input surface of the PMMA phantom,
25 i.e. outside the activated area. Coincidence events are also observed beyond the distal part of the activated area.

After filtering the in-spill data according to the procedure described above, the in-spill inter-bunches data allow obtaining the image shown in figure 7c, where the noise is significantly
30 suppressed.

Figure 8 shows the 1D activity profiles for the inter-spill, in-spill and in-spill inter-bunch

coincidence events (after filtering). In the in-spill case (figure 8b), the background radiation noise is visible in the high activity before the input surface of the phantom and in the tail at the end of the activity range. In figure 8c, the number of coincidence events before the input surface of the phantom decreases significantly while the tail at the end of the activity range does not change significantly.

According to some authors, the activity before the input surface of the phantom is originated by neutrons detected some nanoseconds after the interaction of the beam with the cores (M.A. Piliero et al., 2016, "Full-beam performances of a PET detector with synchrotron therapeutic proton beams", *Phys. Med. Biol.* 61, N650). The signal-to-noise ratio (SNR), given by the activity peak in the phantom divided by the background level, in the inter-bunch in-spill signal is improved by a factor of about 4.8 with respect to the in-spill signal. The tail is probably due to the high range of the short-lived positrons of the β^+ emitters.

CLAIMS

1. Apparatus for acquiring positron emission tomography data when irradiating a target (20) with a hadron beam (B), said apparatus comprising:
- 5 a plurality of detectors (10) configured to detect radiation emitted by the target (20) when irradiating it with the hadron beam (B), and provide detection data; and
- a data processing system (12, 15) configured to reconstruct positron emission tomography imaging data from the detection data provided by the detectors (10), and determine the penetration range of the hadron beam (B) in the target (20);
- 10 characterized in that the data processing system (12, 15) is configured to process the detection data according to the following steps:
- determining a time distribution of the rate of coincidence events acquired by the respective detector (10), said time distribution having a succession of spill intervals correlated with a pulsed time structure of the hadron beam, each spill interval having a micro-structure
- 15 formed by a succession of micro-bunches correlated with a radiofrequency signal of the hadron beam;
- B) sampling each spill interval with a sampling frequency of the order of magnitude of GHz to obtain a respective fine grained event rate distribution;
- c) for each spill interval:
- 20 - c1) analysing frequencies of the fine grained event rate distribution to find an initial frequency value f_0 compatible with the radiofrequency signal of the hadron beam;
- c2) from the initial frequency value, estimating period T_s of the micro-bunches and transforming time values of the coincidence events in the spill interval into values of phase relative to an arbitrary phase, based on the estimated period of the micro-bunches; and
- 25 - c3) at each micro-bunch of the spill interval, executing filtering to remove coincidence events around a peak associated with background noise induced by the hadron beam and keep the remaining coincidence events of the micro-bunch.
2. Apparatus according to claim 1, wherein the step c1) comprises
- 30 calculating a fast Fourier transform of the fine grained event rate distribution.

3. Apparatus according to claim 2, wherein the step c2) comprises
determining, in the fast Fourier transform, the frequency f_0 of the first peak with
non-zero frequency;
determining an initial value T_0 of the period, where $T_0 = 1/f_0$;
5 assigning to each coincidence event a phase value ϕ_i based on the initial value T_0 of
the period such that
$$\phi_i = t_i \bmod T_0, \quad (1)$$

where t_i is the timestamp of the i -th event and mod is the modulus operator; and
iteratively searching for the period T_j around T_0 that maximizes the peak-to-valley
10 ratio of the event rate over the period, to obtain the best estimate T_s of the period of the mi-
cro-bunches.
4. Apparatus according to any of the preceding claims, wherein the step c3) comprises
determining mean μ and standard deviation σ of a Gaussian fit applied to the peak
15 associated with background noise induced by the hadron beam; and
removing the coincidence events comprised in the interval $\mu \pm k\sigma$ where k is an ad-
justable parameter.
5. Apparatus according to any of the preceding claims, wherein the sampling frequen-
20 cy is comprised between 0.01 and 100 GHz.
6. Method for acquiring positron emission tomography data when irradiating a target
(20) with a hadron beam (B), said method comprising:
detecting radiation emitted by the target (20) when irradiating it with the hadron
25 beam (B), and providing detection data; and
reconstructing positron emission tomography imaging data from the provided de-
tection data, and determining the penetration range of the hadron beam (B) in the target
(20);
characterized in that the detection data are processed according to the following
30 steps:
a) determining a time distribution of the rate of acquired coincidence events, said time dis-
tribution having a succession of spill intervals correlated with a pulsed time structure of the

hadron beam, each spill interval having a micro-structure formed by a succession of micro-bunches correlated with a radiofrequency signal of the hadron beam;

b) sampling each spill interval with a

sampling frequency of the order of magnitude of GHz to obtain a respective fine grained event rate distribution;

c) for each spill interval:

- c1) analysing frequencies of the fine grained event rate distribution to find an initial frequency value f_0 compatible with the radiofrequency signal of the hadron beam;

- c2) from the initial frequency value, estimating period T_s of the micro-bunches and transforming time values of the coincidence events in the spill interval into values of phase relative to an arbitrary phase, based on the estimated period of the micro-bunches; and

- c3) at each micro-bunch of the spill interval, executing filtering to remove coincidence events around a peak associated with background noise induced by the hadron beam and keep the remaining coincidence events of the micro-bunch.

15

7. Method according to claim 6, wherein the step c1) comprises calculating a fast Fourier transform of the fine grained event rate distribution.

8. Method according to claim 7, wherein

20 step c2) comprises

determining, in the fast Fourier transform, the frequency f_0 of the first peak with non-zero frequency;

determining an initial value T_0 of the period, where $T_0 = 1/f_0$;

25 assigning to each coincidence event a phase value ϕ_i based on the initial value T_0 of the period such that

$$\phi_i = t_i \bmod T_0, \quad (1)$$

where t_i is the timestamp of the i -th event and mod is the modulus operator; and

iteratively searching for the period T_j around T_0 that maximizes the peak-to-valley ratio of the event rate over the period, to obtain the best estimate T_s of the period of the micro-bunches.

30

9. Method according to any of claims from 6 to 8, wherein the step c3) comprises

determining mean μ and standard deviation σ of a Gaussian fit applied to the peak associated with background noise induced by the hadron beam; and

removing the coincidence events comprised in the interval $\mu \pm k\sigma$, where k is an adjustable parameter.

5

10. Method according to any of claims from 6 to 9, wherein said filtering is further operated as a function of detected energy of the individual coincidence events.

11. Method according to any of claims from 6 to 10, wherein the sampling frequency is

10 comprised between 0.01 and 100 GHz.

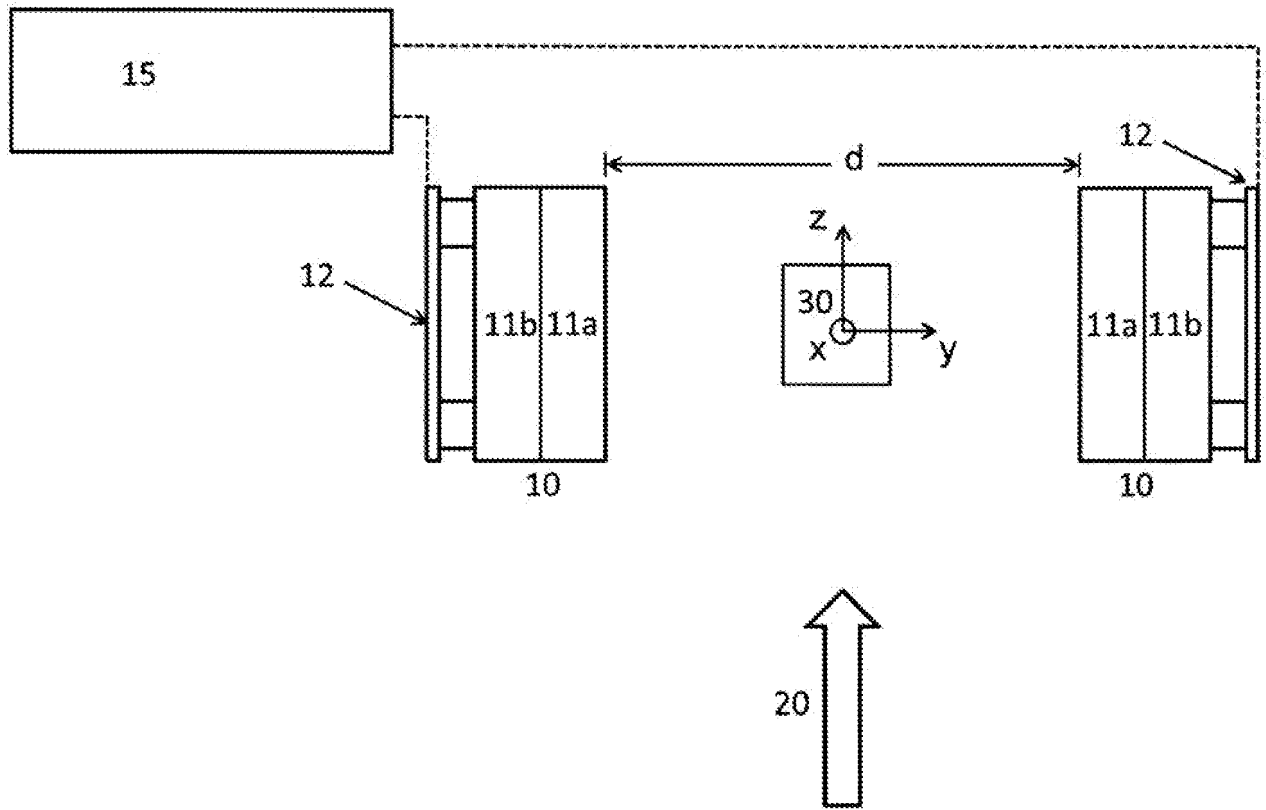


FIG. 1

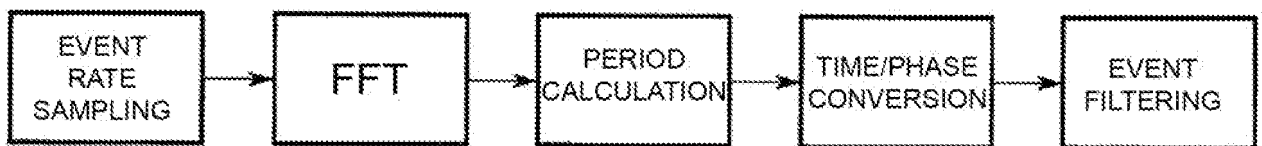


FIG. 2

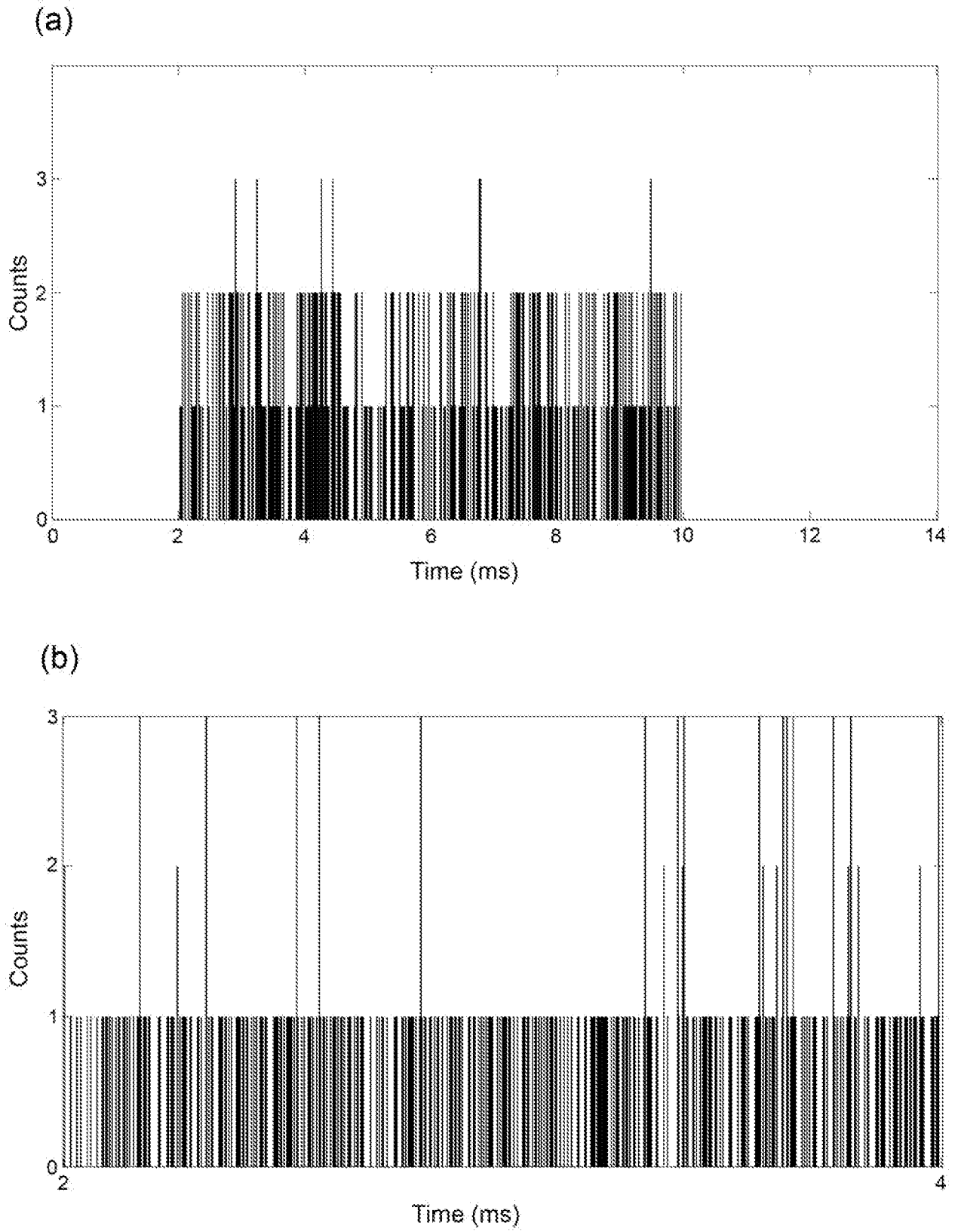


FIG. 3

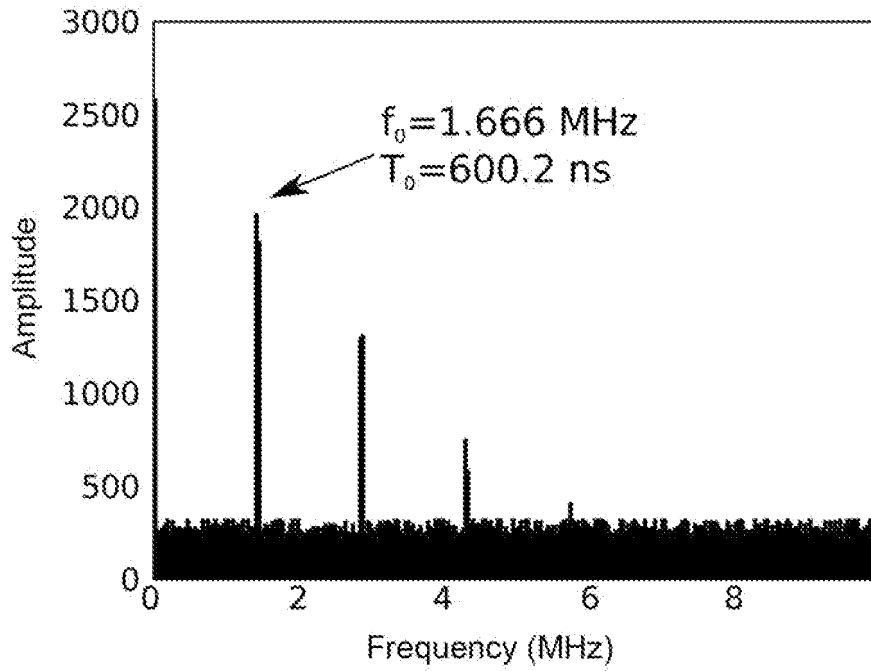


FIG. 4

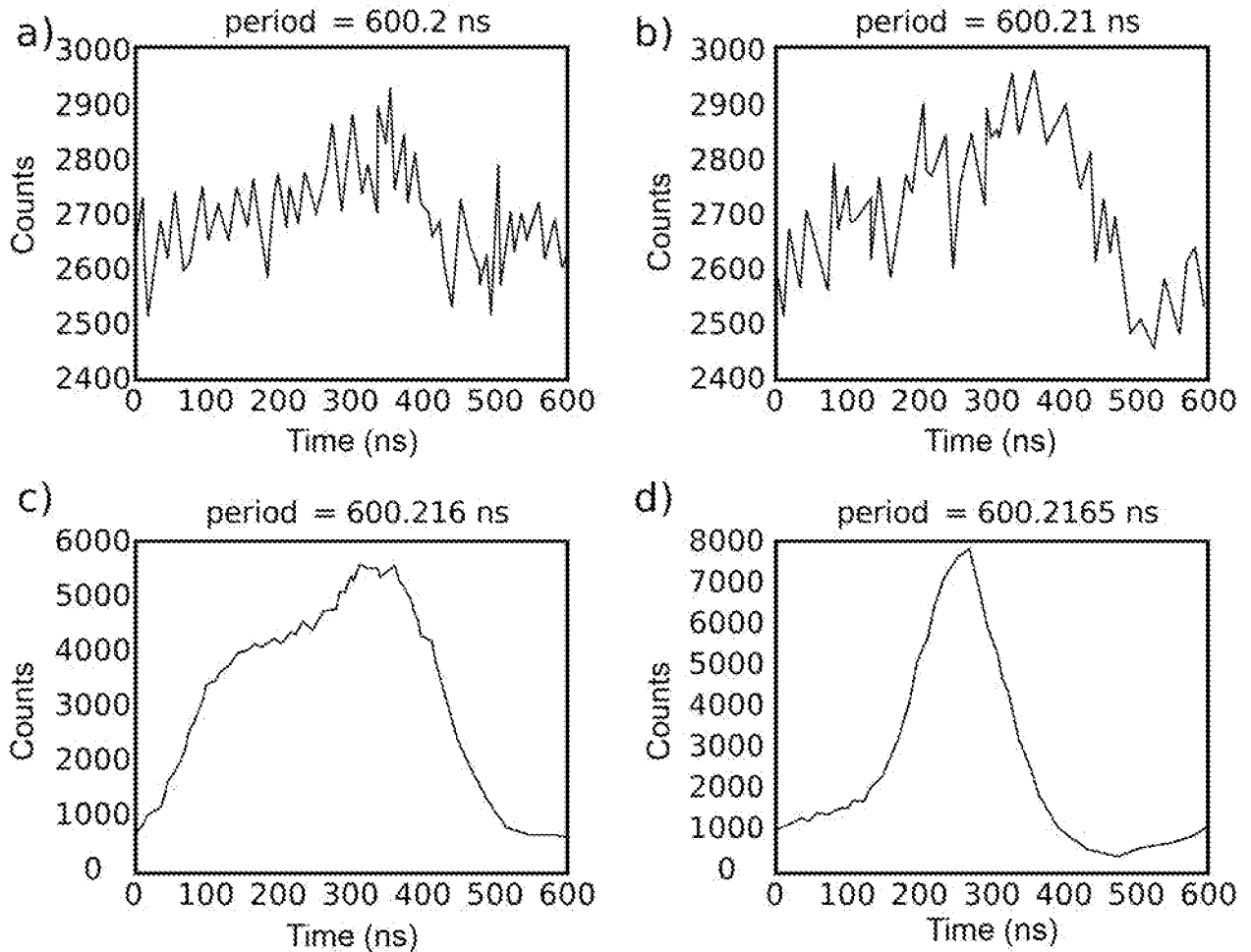


FIG. 5

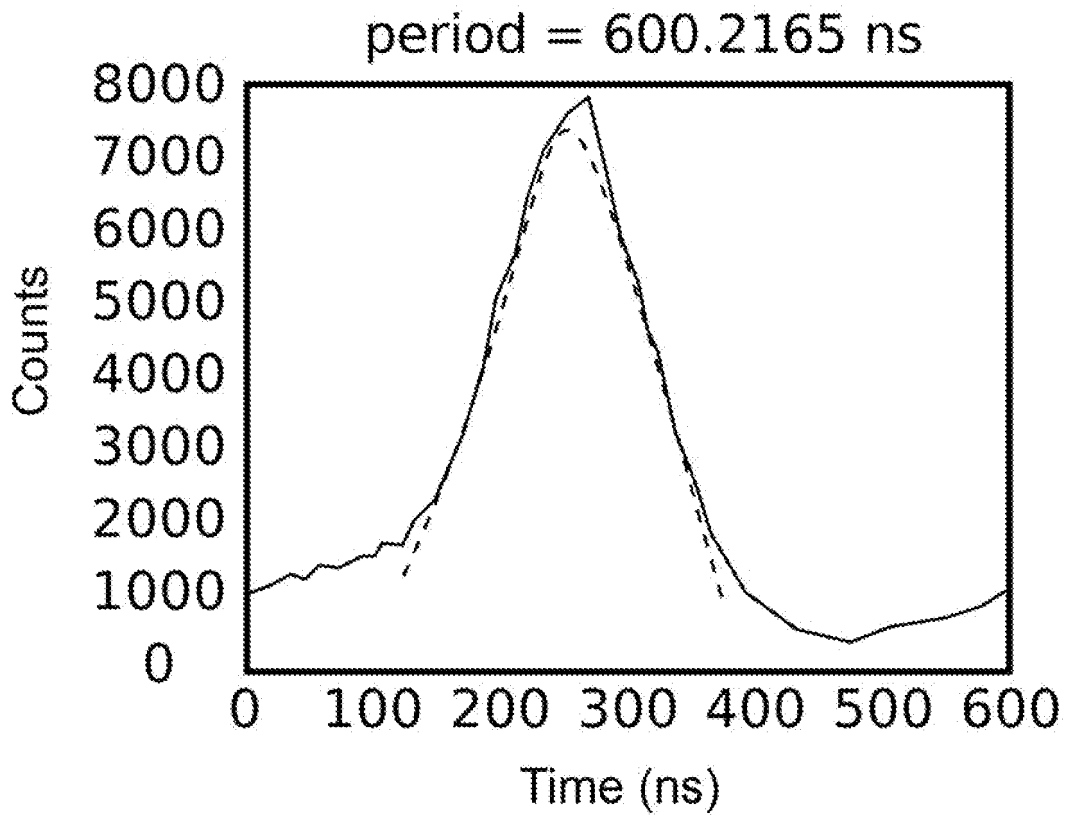


FIG. 6

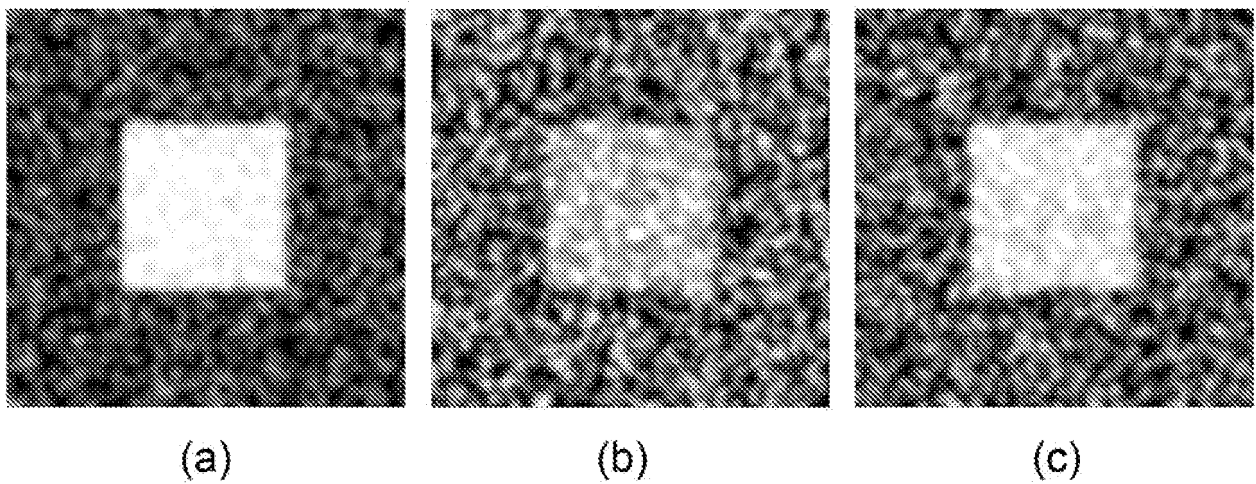


FIG. 7

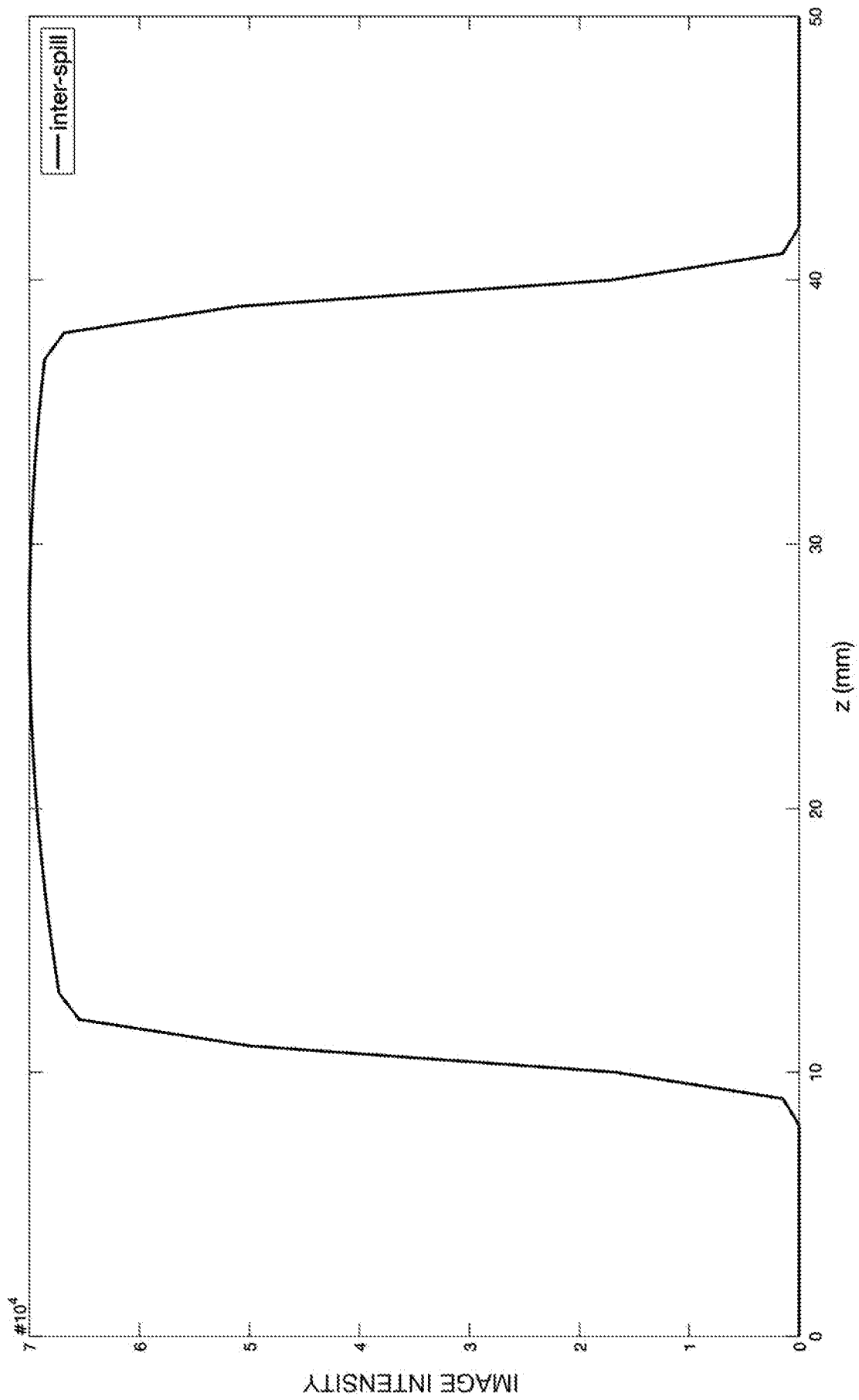


FIG. 8a

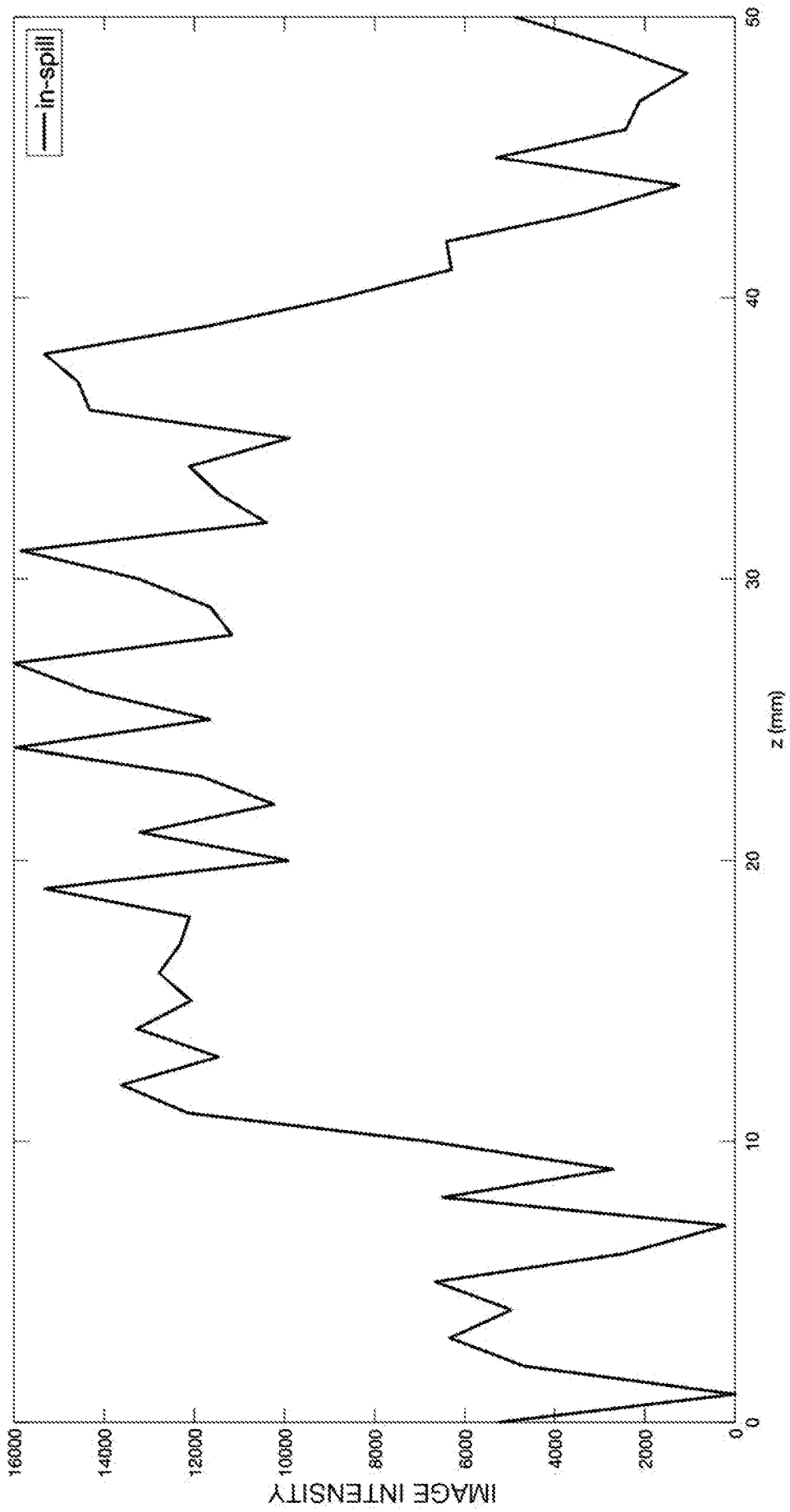


FIG. 8b

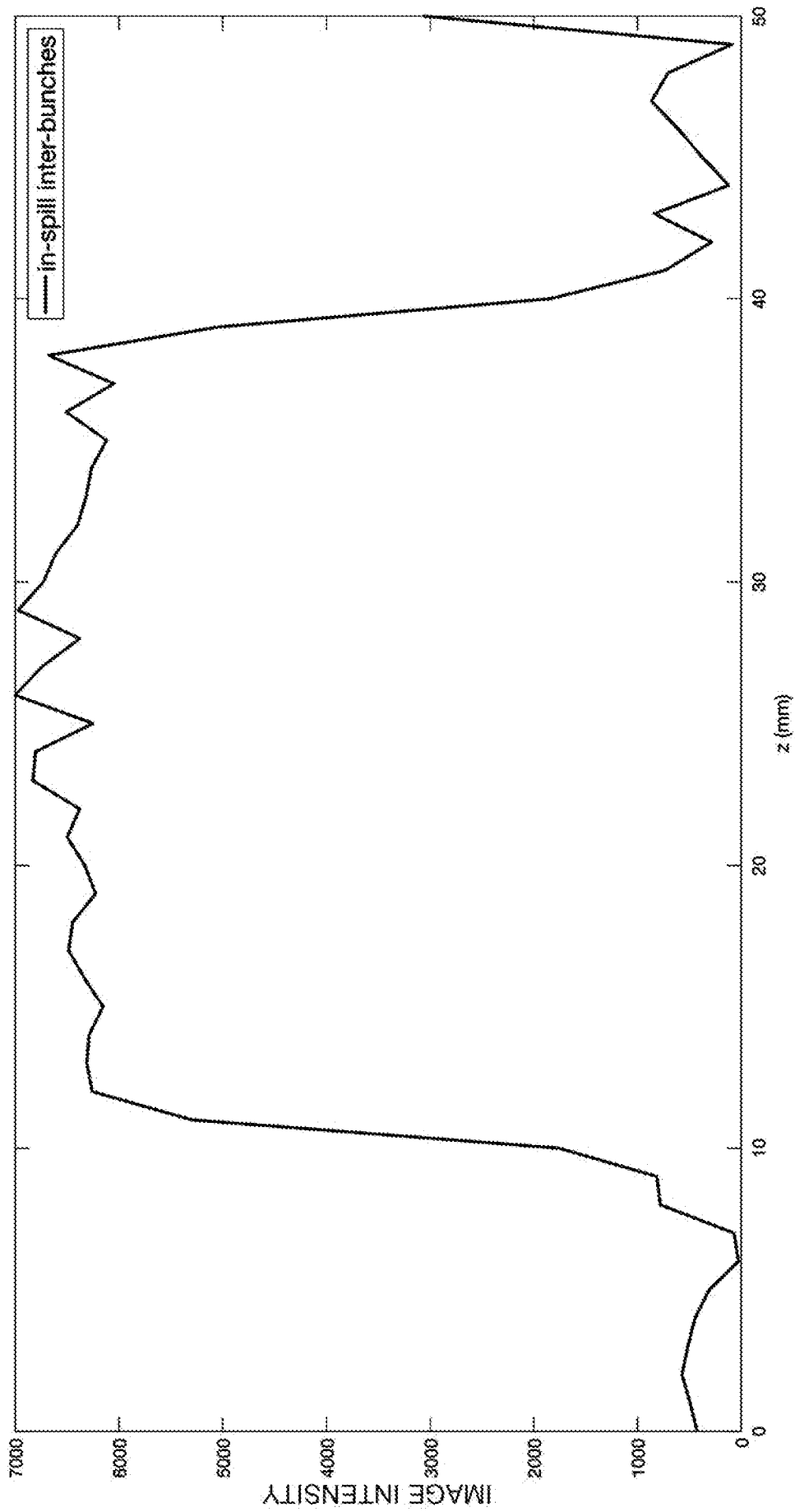


FIG. 8C

INTERNATIONAL SEARCH REPORT

International application No
PCT/IB2019/050258A. CLASSIFICATION OF SUBJECT MATTER
INV. G01T1/29 A61N5/10
ADD.

According to International Patent Classification (IPC) or to both national classification and IPC

B. FIELDS SEARCHED

Minimum documentation searched (classification system followed by classification symbols)
G01T A61N

Documentation searched other than minimum documentation to the extent that such documents are included in the fields searched

Electronic data base consulted during the international search (name of data base and, where practicable, search terms used)

EPO-Internal, INSPEC, COMPENDEX

C. DOCUMENTS CONSIDERED TO BE RELEVANT

Category*	Citation of document, with indication, where appropriate, of the relevant passages	Relevant to claim No.
A	LESTAND LOIC ET AL: "In Beam PET Acquisition on 75 MeV. u^{-1} Carbon Beam Using Sampling-Based Read-Out Electronics", IEEE TRANSACTIONS ON RADIATION AND PLASMA MEDICAL SCIENCES, IEEE, vol. 1, no. 1, 1 January 2017 (2017-01-01), pages 87-95, XP011642479, ISSN: 2469-7311, DOI: 10.1109/TNS.2016.2635584 [retrieved on 2017-03-06] abstract; figures page 87, paragraph I. page 88, paragraph II.B - page 89 page 90, paragraph II.E - paragraph II.F ----- -/--	1-11

 Further documents are listed in the continuation of Box C. See patent family annex.

* Special categories of cited documents :

"A" document defining the general state of the art which is not considered to be of particular relevance

"E" earlier application or patent but published on or after the international filing date

"L" document which may throw doubts on priority claim(s) or which is cited to establish the publication date of another citation or other special reason (as specified)

"O" document referring to an oral disclosure, use, exhibition or other means

"P" document published prior to the international filing date but later than the priority date claimed

"T" later document published after the international filing date or priority date and not in conflict with the application but cited to understand the principle or theory underlying the invention

"X" document of particular relevance; the claimed invention cannot be considered novel or cannot be considered to involve an inventive step when the document is taken alone

"Y" document of particular relevance; the claimed invention cannot be considered to involve an inventive step when the document is combined with one or more other such documents, such combination being obvious to a person skilled in the art

"&" document member of the same patent family

Date of the actual completion of the international search

18 March 2019

Date of mailing of the international search report

10/04/2019

Name and mailing address of the ISA/

European Patent Office, P.B. 5818 Patentlaan 2
NL - 2280 HV Rijswijk
Tel. (+31-70) 340-2040,
Fax: (+31-70) 340-3016

Authorized officer

Eberle, Katja

INTERNATIONAL SEARCH REPORT

International application No
PCT/IB2019/050258

C(Continuation). DOCUMENTS CONSIDERED TO BE RELEVANT

Category*	Citation of document, with indication, where appropriate, of the relevant passages	Relevant to claim No.
A	<p>PARODI K ET AL: "Random coincidences during in-beam PET measurements at microbunched therapeutic ion beams", NUCLEAR INSTRUMENTS & METHODS IN PHYSICS RESEARCH. SECTION A, ELSEVIER BV * NORTH-HOLLAND, NL, vol. 545, no. 1-2, 11 June 2005 (2005-06-11), pages 446-458, XP027781751, ISSN: 0168-9002 [retrieved on 2005-06-11] abstract; figures page 452, paragraph 4. - page 453 -----</p>	1-11
A	<p>BARTHEL T ET AL: "Suppression of Random Coincidences During In-Beam PET Measurements at Ion Beam Radiotherapy Facilities", IEEE TRANSACTIONS ON NUCLEAR SCIENCE, IEEE SERVICE CENTER, NEW YORK, NY, US, vol. 52, no. 4, 1 August 2005 (2005-08-01), pages 980-987, XP011137769, ISSN: 0018-9499, DOI: 10.1109/TNS.2005.852637 abstract -----</p>	1-11